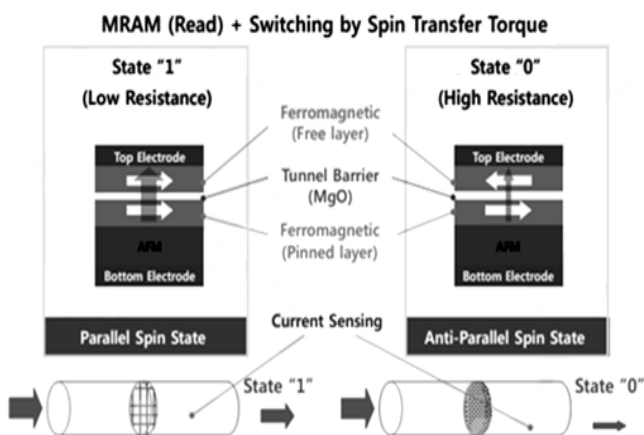


Basic

Structure of a STT Cell

1.2 Introduction to MRAM and STT Technologies

Magnetoresistive Random Access Memory (MRAM) is a technology that has existed in various forms since the late 1970s. MRAM is based on the concept of using the direction of magnetization to store binary information, while exploiting magnetoresistive properties for data retrieval. The mid-1990s saw a resurgence of interest in MRAM technologies with the discovery of room temperature tunneling magnetoresistance (TMR) in magnetic tunnel junctions (MTJs). A magnetic tunnel junction (MTJ) is simply to be understood as a pair of ferromagnetic layers (Top layer / electrode – Free Layer & Bottom layer / electrode – Pinned layer) separated by a thin insulating layer, which acts like a tunnel-barrier. Two possible magnetic states arise, the parallel combination of the two layers (Fig. 1.2(a)) and the antiparallel combination (Fig. 1.2(b)). The parallel configuration leads to a low resistive state (R_P), while the antiparallel configuration leads to a high resistive state (R_{AP}).



$R_P R_{AP}$ Two possible magnetic switching states of STT MRAM

Spintronics, the amalgamation of the words “spin” and “electronics”, involves the active control and manipulation of electron spin in solid-state electronics. In traditional electronic devices, information processing works on the principle of control over the flow of charge through a semiconductor material. Large scale, non-volatile memories (e.g., hard disk drives or HDDs) exploit ferromagnetism to store information by forcing the spin alignment of many electrons. Spintronics, as a whole, aims to merge information processing and storage through the use of spin-polarized currents. An important adverse effect of GMR (Giant Magnetoresistance): Spin-Transfer effect, in which magnetization orientations (corresponding to low-high resistance states) in magnetic multilayer nanostructures can be manipulated via spin polarized current was first theoretically predicted and demonstrated by J.C.Slonczewski and Berger in 1996. This has formed the basis of next generation MRAMs. STT-MRAM can scale well below 65nm, while reducing writing currents by more than a hundredfold. Before STT, writing currents increased exponentially with MRAM scaling, causing electromigration and power concerns that prevented scaling below 90nm. The nonvolatile nature, low power, high performance, and memory density of STT-MRAM make it an excellent candidate for the first commercially available universal memory. However, the lack of an accurate, compact macro-model, incorporating temperature and bias voltage effects, is the largest obstacle to the design of high performance STT-MRAMs. Without such a design tool, it is impossible to verify timing and yield or predict device behavior with scaling. Another big challenge is the integration of MTJs with CMOS. Although the process flow is in principle fully compatible with CMOS, adds extra design and layout constraints.

In literature, Spin-Torque Transfer Random Access Memory (STT-RAM) and Spin Random Access Memory (SPRAM) are used interchangeably with STT-MRAM. However, STT-MRAM is more common and is, therefore, used exclusively in this paper.

1.3 Principle of Operation

Electron spin is a “pseudovector” with fixed magnitude but a variable direction (spin polarization). The spin polarization of an electron can be made bistable by placing it in a magnetic field. In the presence of a magnetic field, only spin polarizations parallel or antiparallel to the field are possible. The effect of spin transfer torque in MTJs can be studied with the advent of STT vector, driven by linear response voltage, computed from the expectation value of the torque operator:
$$\mathbf{T} = \text{Tr}[\hat{\mathbf{T}} \hat{\rho}_{\text{neq}}]$$

where $\hat{\rho}_{\text{neq}}$ is the gauge-invariant nonequilibrium density matrix for the steady-state transport, in the zero-temperature limit, in the linear-response regime, and the torque operator is obtained from the time derivative of the spin operator:

$$\hat{T} = \frac{d\hat{S}}{dt} = -\frac{i}{\hbar} \left[\frac{\hbar}{2} \sigma, \hat{H} \right]$$

Using the general form of a 1D tight-binding Hamiltonian:

$$\hat{H} = \hat{H}_0 - \Delta(\sigma \cdot \mathbf{m})/2$$

where total magnetization (as macrospin) is along the unit vector \mathbf{m}

The STT vector in general MTJs has two components: a parallel and perpendicular component:

A parallel component: $T_{||} = \sqrt{T_x^2 + T_z^2}$

And a perpendicular component: $T_{\perp} = T_y$

While in symmetric MTJs (made of electrodes with the same geometry and exchange splitting), the STT vector has only one active component, as the perpendicular component disappears:

Therefore, we have $T_{||}$ vs. θ needs to be plotted at the site of the right electrode to characterise tunnelling in symmetric MTJs, making them appealing for industrial scale production and characterisation.

1.4 The Magnetic Tunnel Junction (MTJ) – Characteristics

Resistance Hysteresis, Critical Switching Current, Temperature Dependence, Bias Voltage Effects, Self Induced Heating, Backhopping and Noise are the important characteristics which feature the operation of a MTJ. The greatest hindrance in the design of STT-MRAMs and other Spintronic Circuits with metals and metal composites is the lack of compact MTJ model, capable of accurately modeling temperature and voltage dependencies. Hence in this connection, the current paper tries to figure out “ Spin life time ” or “ Current pulse width ” as the responsible physical parameter, hindering the performance and scalability of STT-MRAMs and other spintronic circuits. The magnetization dynamics in a MTJ is as follows: The precessional motion of magnetization of the

free layer of a MTJ, in the presence of an effective magnetic field, can be very accurately modeled by the Landau-Lifshitz-

$$\frac{\partial \vec{m}}{\partial t} = -\gamma M_S \vec{m} \times \left(\vec{H}_{eff} - \alpha \frac{\partial \vec{m}}{\partial t} \right)$$

Gilbert equation (LLGE)

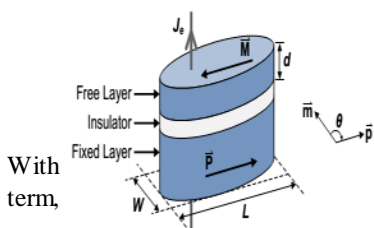


Figure : Schematic of basic MTJ structure.

with term, τ is given by:

$$\frac{\partial \vec{m}}{\partial t} = -\gamma M_S \vec{m} \times \left(\vec{h}_{eff} + \frac{J_e}{J_C} b(\theta) (\vec{m} \times \vec{p}) - \alpha \frac{\partial \vec{m}}{\partial t} \right),$$

where $(\gamma_e \mu_B)$, m is the absolute value of the gyromagnetic ratio is the unit vector in the direction of \vec{M} , \vec{p} , $\vec{h}_{eff} = \vec{H}_{eff}/M_S$, J_e is the unit vector in the direction of the magnetization of the fixed layer is the current density (see Fig), θ is the angle between \vec{m} and \vec{p} and is the material-dependent Gilbert damping constant. The factor of spin-polarization $b(\theta)$ is defined as:

$$b(\theta) = \left[-4 + (1 + P)^3 \frac{3 + \cos(\theta)}{4P^{3/2}} \right]^{-1},$$

where P is the percentage of electrons polarized in the direction, (J_C) switching current density has been modified to include thermally-activated switching. For a constant pulse of duration τ is given by:

$$J_C = J_{C0} \left[1 - \frac{\ln(\tau/\tau_0)}{\Delta} \right],$$

where $\Delta = \frac{K_u V}{k_B T}$ is the thermal stability of the MTJ and τ_0 is the natural time constant and is the inverse of the attempt frequency, $K_u V$ is the anisotropy energy. Furthermore, the characteristic current density (J_{C0}) defined as:

$$J_{C0} = \gamma M_S \frac{e M_S d}{g_e \mu_B},$$

where e is the absolute value of charge of electron, d is the thickness of the free layer, g_e is the Lande's g factor for electrons and μ_B is the Bohr magneton.

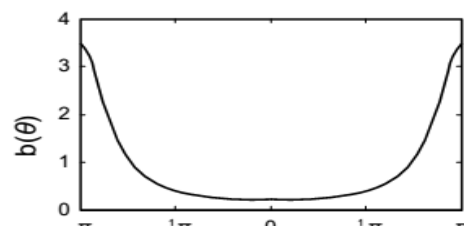


Figure : Magnitude of the efficiency factor of spin-polarization vs. θ for

The effective magnetic field is given by:

$$\vec{H}_{eff} = \vec{H}_{ext} + \vec{H}_{dem} + \vec{H}_{an}$$

Where \vec{H}_{ext} is the external applied magnetic field, \vec{H}_{dem} is the demagnetization field, and \vec{H}_{an} is the magnetocrystalline anisotropy field. The demagnetization field (shape anisotropy)

varies with the geometry of the free layer and is modeled as If the free layer is assumed to be a very flat ellipsoid, the factors of the demagnetization tensor N, calculated

by Osborn are:

$$N_x = \frac{d}{L} (1 - e^2)^{1/2} \frac{K - E}{e^2},$$

$$N_y = \frac{d}{L} \frac{K - (1 - e^2) E}{e^2 (1 - e^2)^{1/2}},$$

$$N_z = 1 - \frac{d}{L} \frac{E}{(1 - e^2)^{1/2}},$$

Where K and E are the complete elliptic integrals of the first and second kind whose argument is

$$e = (1 - W^2/L^2)^{1/2}.$$

The temperature dependencies are given as follows:

In the dynamic equations, only the magnetization saturation (M_s) and the spin-polarization (P) vary with temperature. For temperatures below the Curie temperature (T_C), we can use the Weiss theory of ferromagnetism to model:

$$M_s(T) = M_{s0}(1 - T/T_C)^\beta,$$

Where M_{s0} is the magnetization saturation at absolute zero and β is the material-dependent critical exponent. Similarly the temperature dependence of spin-polarization has been extensively studied and shown to be:

$$P(T) = P_0(1 - \alpha_{sp}T^{3/2})$$

Where P_0 is the spin-polarization at absolute zero and is a material and geometric dependent constant.

From the magnetization dynamics of MTJ, it is clear that

$$\Delta = \frac{K_u V}{K_B T} \quad \text{the thermal stability of MTJ is a temperature}$$

dependent parameter, can be altered so as to effect and enhance the spin life time τ in metals and metal composites.

With the advent of applying Ultracold Plasmas, the temperature parameter in the denominator of thermal stability factor can be brought about to several nano Kelvin (nK), thereby which an extensive macroscopic increase in the thermal stability of the MTJ is visualised, which in turn enhances the spin life time τ in the logarithmic term in switching current density.

1.5 Introduction to Ultracold Plasma & characteristic Temperature

Ultracold plasmas, produced by photoionizing a sample of laser-cooled and trapped atoms near the ionization limit, have extended traditional neutral plasma parameters by many orders of magnitude, to electron temperatures below 1 K and ion temperatures in the tens of μK to a few Kelvin, and densities of 10^5 cm^{-3} to 10^{10} cm^{-3} . These plasmas thus provide a testing ground to study basic plasma theory in a clean and simple system with or without a magnetic field. Previous studies of ultracold plasmas have primarily

concentrated on temperature measurements, collective modes and expansion dynamics in the absence of magnetic fields. This paper presents the first study of ultracold plasma dynamics in a magnetic field in enhancing the spin life time τ via a significant change being produced in the electron temperature in thermal stability factor in MTJ. The presence of a magnetic field during the expansion can initiate various phenomena, such as plasma confinement and plasma instabilities. While the electron temperatures are very low in ultracold plasmas, we need only tens of Gauss of magnetic field to observe significant effects on the expansion dynamics.

Plasma temperature is commonly measured in Kelvins or electronvolts and is, informally, a measure of the thermal kinetic energy per particle. Very high temperatures are usually needed to sustain ionization, which is a defining feature of a plasma. The degree of plasma ionization is determined by the "electron temperature" relative to the ionization energy (and more weakly by the density), in a relationship called the Saha equation. At low temperatures, ions and electrons tend to recombine into bound states—atoms and the plasma will eventually become a gas. In most cases the electrons are close enough to thermal equilibrium that their temperature is relatively well-defined, even when there is a significant deviation from a Maxwellian energy distribution function.

1.6 Road to reduce Spin Transfer switching current i.e the Spin life time via Ultracold Plasma technologies

Manipulation of the thin film magnetization by transferring spin angular momentum from a spin-polarized current in nanomagnets both to drive precessional dynamics and to trigger magnetization reversal presents promising opportunities for better and magnetic memory devices such as magnetic random access memory (MRAM). However scalability characteristics in nanoscale microwave oscillators one of the major practical concerns is the current level needed to write magnetic bits in an error-free fashion at high operating speeds. This indeed poses a limit on the areal density one could achieve in a memory circuit using spin transfer because the required current level determines the size of the change in this feature will be expected by ultracold plasma write transistor needed. This potential technological applicability has triggered an intense effort to optimize the device geometry and choice of materials to obtain reduction in switching currents. A significant technologies like Inductively coupled plasma, Capacitively coupled plasma and

UGC Sponsored National Conference on

Advanced Technology Oriented Materials (ATOM-2014), 8-9th Dec-2014

Department of Physics, Government College (A), Rajahmundry, Andhra Pradesh, India

Cascaded Arc Plasma Source, which surely result in the considerable reduction of spin transfer switching current or the spin life time τ , which results in better performance and scalability of STT-MRAMs.

1.7 Several Ultracold Plasma technologies

1. Inductively coupled plasma: An inductively coupled plasma (ICP) is a type of plasma source in which the energy is supplied by electric currents which are produced by electromagnetic induction, that is, by time-varying magnetic fields. Plasma temperatures can range between $\sim 6000\text{ K}$ and $\sim 10000\text{ K}$ ($\sim 1\text{ eV}$ - $\sim 100\text{ eV}$), comparable to the surface of the sun. ICP discharges are of relatively high electron density, on the order of 10^{15} cm^{-3} . As a result, ICP discharges have wide applications where a high-density plasma (HDP) is needed. Another benefit of ICP discharges is that they are relatively free of contamination because the electrodes are completely outside the reaction chamber. By contrast, in a capacitively coupled plasma (CCP), the electrodes are often placed inside the reactor and are thus exposed to the plasma and subsequent reactive chemical species.

2. Capacitively coupled plasma : A capacitively coupled plasma (CCP) is one of the most common types of industrial plasma sources. It essentially consists of two metal electrodes separated by a small distance, placed in a reactor. The gas pressure in the reactor can be lower than atmosphere or it can be atmospheric. A typical CCP system is driven by a single radio-frequency (RF) power supply, typically at 13.56 MHz. One of two electrodes is connected to the power supply, and the other one is grounded. As this configuration is similar in principle to a capacitor in an electric circuit, the plasma formed in this configuration is called a capacitively coupled plasma.

When an electric field is generated between electrodes, atoms are ionized and release electrons. The electrons in the gas are accelerated by the RF field and can ionize the gas directly or indirectly by collisions, producing secondary electrons. When the electric field is strong enough, it can lead to what is known as electron avalanche. After avalanche breakdown, the gas becomes electrically conductive due to abundant free electrons. Often it accompanies light emission from excited atoms or molecules in the gas. When visible light is produced, plasma generation can be indirectly observed even with bare eyes.

A variation on capacitively coupled plasma involves isolating one of the electrodes, usually with a capacitor. The capacitor appears like a short circuit to the high frequency RF field, but like an open circuit to DC field. Electrons impinge on the electrode in the sheath, and the electrode quickly acquires a negative charge (or self-bias) because the capacitor does not allow it to discharge to ground. This sets up a secondary, DC field across the plasma in addition to the AC field. Massive ions are unable to react to the quickly changing AC field, but the strong, persistent DC field accelerates them toward the self-biased electrode. These energetic ions are exploited in many microfabrication processes (see RIE) by placing a substrate on the isolated (self-biased) electrode.

CCPs have wide applications in the semiconductor processing industry for thin film deposition (sputtering, Plasma-enhanced chemical vapor deposition {PECVD}) and etching.

3. Cascaded Arc Plasma Source: The cascaded arc is a wall-stabilized thermal electric arc discharge that produces a high density, low temperature plasma. The cascaded arc source, developed at the Eindhoven University of Technology. Compared to plasma sources in other linear plasma generators, this source can produce high-density argon and hydrogen plasmas (respectively 10^{21} - 10^{24} m^{-3} and 10^{19} - 10^{22} m^{-3}) at a relatively low electron temperature ($\sim 1\text{ eV}$). Due to the high collision frequency of the particles in the source, the plasma is in thermal equilibrium and reasonably homogeneous.

The cascaded arc consists of a gas inlet, three tungsten cathodes, cascaded plates, a nozzle and an anode. Via the gas inlet, the working gas -argon or hydrogen- can flow into the cathode chamber. The source is typically running at 0.5 - 3.0 Standard Liter Per Minute (slm). (1 Standard Liter Per Minute = $4.4 \cdot 10^{20}$ particles per second) and a discharge current of 100-300 A. The cascaded plates in between the cathode and anode are electrically insulated from each other by 1 mm thick Boron nitride plates. The voltage of these plates is the floating potential. Both nozzle and anode are grounded.

3. References

- [1] J C. Slonczewski, *J. Magn. Mater.* 159 L 1, 1996.
- [2] Berger L, *Phys. Rev. B* 54 pp. 9359, 1996.
- [3] J C. Slonczewski, *J. Magn. Mater. Pp.* 247 324, 2002. Slonczewski J C 2005 *Phys. Rev. B* 71 024411
- [4] X Waintal, E B. Myers, P W. Brouwer and D C. Ralph *Phys. Rev. B* 62 12317, 2000.
- [5] R W Dorrance Modeling and Design of STT-MRAMs Thesis Submitted for partial Of Master of Sciene in Electrical Engineering, UCLA 2011
- [6] Zhitao Diao, Zhanjie Li, Shengyuang Wang, Yunfei Ding, Alex Panchula, Eugene Chen, Lien-Chang Wang and Yiming Huai *J Phys: Condens. Matter* 19, pp.165-209, 2007.
- [7] Yiming Huai AAPPS Bulletin, Vol. 18, No.6, December 2008
- [8] Roy O. Wilson and A. Duncan. Tate BAPS..DAMOP.D1.8, 2007.
- [9] P. Gupta, S. Laha, C. Simien, H. Gao, J. Castro, T. C. Killian, "Electron-Temperature Evolution in Expanding Ultracold Neutral Plasmas", *Phys. Rev. Lett.*, 99, 075005, 2007.
- [10] Rishubh Garg, Jyothi Kedia UJPA 1(3):pp. 290-94, 2013.
- [11] C. M Braams *Phys. Rev.* 17 (9): 470
- [12] Pershin Y. V., Di Ventra M., *Phys. Rev. B* 78 (11) 113309, 2008.
- [13] M. Julliere *Phys. Rev.* 54A 225-226, 1975.
- [14] T. Miyazaki and N. Tezuka (1995) *J. Magn. Mater.* 139 L231-L234
- [15] J. S. Moodera *et al. Phys. Rev.* 74 (16): pp.3273-3276, 1995.
- [16] S Yuasa, T Nagahama, A Fukushima, Y Suzuki and K Ando *Nat. Mat.* 3(12), 2004.
- [17] S. S. P. Parkin *et al. Nat. Mat.* 3(12), pp.862-867, 2004.
- [18] F. Mahfouzi, N. Nagaosa, and B.K. Nikolic *Phys. Rev.* 109, pp.166-602 2012.
- [19] S-C. Oh *et. al, Nature Phys.*, 5, pp. 898, 2009.
- [20] W. H. Butler, X. G. Zhang, T. C. Schulthess, J. M. MacLaren *Phys. Rev. B* 63 (5), 2001.